ACS APPLIED MATERIALS & INTERFACES

Research Article

www.acsami.org

Hybrid Theranostic Platform for Second Near-IR Window Light Triggered Selective Two-Photon Imaging and Photothermal Killing of Targeted Melanoma Cells

Christine Tchounwou, Sudarson Sekhar Sinha, Bhanu Priya Viraka Nellore, Avijit Pramanik, Rajashekhar Kanchanapally, Stacy Jones, Suhash Reddy Chavva, and Paresh Chandra Ray*

Department of Chemistry and Biochemistry, Jackson State University, Jackson, Mississippi 39217, United States

Supporting Information

ABSTRACT: Despite advances in the medical field, even in the 21st century cancer is one of the leading causes of death for men and women in the world. Since the second near-infrared (NIR) biological window light between 950 and 1350 nm offers highly efficient tissue penetration, the current article reports the development of hybrid theranostic platform using anti-GD2 antibody attached gold nanoparticle (GNP) conjugated, single-wall carbon nanotube (SWCNT) for second near-IR light triggered selective imaging and efficient photothermal therapy of human melanoma cancer cell. Reported results demonstrate that due to strong plasmon-coupling, two-photon luminescence (TPL) intensity from theranostic GNP attached SWCNT materials is 6 orders of magnitude higher than GNP or SWCNT alone. Experimental and FDTD simulation data indicate that the huge enhancement of TPL intensity is mainly due to strong resonance enhancement coupled with the stronger electric field enhancement. Due to plasmon coupling, the theranostic material serves as a local nanoantennae to enhance the photothermal capability via strong optical energy absorption. Reported data show that theranostic SWCNT can be used for selective two-photon imaging of melanoma UACC903 cell using 1100 nm light. Photothermal killing experiment with 1.0 W/cm^2 980 nm laser light demonstrates that 100% of melanoma UACC903 cells can be killed using theranostic SWCNT bind melanoma cells after just 8 min of exposure. These results demonstrate that due to plasmon coupling, the theranostic GNP attached SWCNT material serves as a two-photon imaging and photothermal source for cancer cells in biological window II.

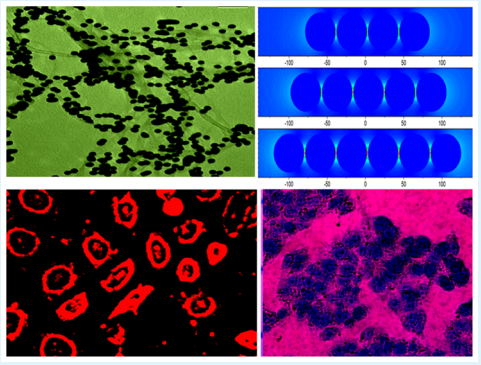

KEYWORDS: *theranostic platform, hybrid plasmonic CNT, second biological window, FDTD simulation, two-photon imaging of human melanoma cancer cell, selective photothermal therapy*

INTRODUCTION

Targeted imaging and light induced photothermal therapy using near-infrared (NIR) light at the second biological window will be the best option to decrease mortality from cancer.[1−6] Theranostic nanoplatform with combined diagnostic and therapeutic functions promise personalized nanomedicine for cancer.[2−10] It is now well documented that near-infrared (NIR) light between 750 and 2400 nm can penetrate biological tissues and blood more efficiently.[5−13] As a result, for in vivo bright cancer imaging and effective light induced photothermal therapy, first and second NIR biological window light will be the best option for clinical study.[5−13] Due to the larger penetration depth through skin, tissues, and blood, second NIR biological window light between 1000 and 1250 nm will be a better choice than the first biological window.[10−16] Despite huge advances in discovering various types of fluorescence probes, single-photon fluorescence imaging for biomolecules using second biological NIR light remains a huge challenge.[15−21] Two-photon luminescence (TPF) imaging has been introduced in biology and clinical study to solve the above problem.[15−24] But, finding photostable TPF material that exhibits strong two-photon luminescence efficiency in biological window II is rare.[20−28] The current article reports plasmon-coupling enhanced, bright two-photon imaging of melanoma UACC903 cells in biological II window using anti-GD2 antibody attached gold nanoparticle (GNP) conjugated single-wall carbon nanotubes (SWCNTs).

Over the past few years it is well documented that bioconjugated gold nanoparticles are highly photostable, where photoblinking and photobleaching are minimum during two-photon imaging.[4−7,11,15,17−22] As a result, aptamer/antibody or peptide-conjugated gold nanoparticles are very good candidates for bioimaging in clinical environment.[4−7,11,15,17−22] Similarly, we and others have reported that, due to high yield production at low cost, carbon nanomaterials like SWCNTs hold great promise for various applications for our

Received: June 12, 2015
Accepted: September 1, 2015
Published: September 1, 2015

DOI: 10.1021/acsami.5b05225
ACS Appl. Mater. Interfaces 2015, 7, 20649−20656

society.[8−10,12,23,24] Since spherical gold nanoparticles do not have absorption in the second biological window, here we have used two-photon luminescence spectroscopy to image melanoma cell selectively. To achieve the goal of very bright two-photon imaging of melanoma UACC903 cells, plasmon coupling between metal nanoparticles on SWCNTS template has been used to dramatically enhance the two-photon luminescence properties via enhanced light−matter interaction through plasmon-coupling in "hot spot", formed by GNP on the surface of theranostic SWCNTs. In the theranostic nanomaterials, SWCNTs are used as templates for the controlled attachment of gold nanoparticles, which are in close contact, as shown in Figure 1. As a result, several "hot" sites are generated on theranostic SWCNT surface to increase the local E-fields heavily, which enhances the TPL signal significantly. Since it is well documented that the tumor-associated ganglioside GD2 is overexpressed in melanomas,[16] for the purpose of selective imaging of melanoma cell, we have performed anti-GD2 antibody attachment to the nanomaterials via GNP assembly. Selectivity has been demonstrated by performing identical experiments using s normal skin cell line, human skin HaCaT keratinocytes.

Melanoma has been responsible for more than 75% of skin cancer-related deaths in the last few decades.[25] Since melanoma is well-known to be an aggressive form of skin cancer that is highly resistant to conventional therapies,[13,25] anti-GD2 antibody attached theranostic SWCNT material can be used for targeted photothermal killing of this malignant cancer. In the last few years, it is well documented that gold nanoparticles are capable of efficient heat generation under illumination with laser radiation.[8,10−13] Clinicians are considering that photothermal optical treatment is an emerging method of treatment for cancer.[8,10−13] To date, most of the photothermal therapy reported so far involves killing of cancer cells using biological I window (650−850 nm) NIR light.[2−4,8,11,26−30] Driven by the need to find theranostic material which can be used for photothermal killing in the second biological window, this article reports that anti-GD2 antibody attached, gold nanoparticle decorated SWCNTs have the capability to kill 100% of melanoma UACC903 cells using 980 nm light. Since antibody conjugated, gold nanoparticle coated SWNTs exhibit strong NIR absorption through plasmon coupling, reported photothermal killing results demonstrate that 8 min of photothermal treatment by 1.0 W/cm^2 980 nm laser light using laser diode is enough to kill melanoma UACC903 cells very effectively.

MATERIALS AND EXPERIMENTS

Synthesis of Anti-GD2 Antibody Attached Gold Nanoparticle. Spherical GNPs of around 40 nm size were synthesized from gold chloride ($HAuCl_4$, $3H_2O$) and sodium citrate using our reported procedure.[4,5,8,13,23] In the next step, to synthesize the anti-GD2 antibody conjugated GNP, at first we have modified the 40 nm GNP surface with cystamine dihydrochloride. After that, we have performed covalent immobilization of the anti-GD2 antibody onto the amine group of cystamine dihydrochloride conjugated GNP using glutaraldehyde spacer method as reported previously.[31] For this purpose, at first, 5 mL of cystamine dihydrochloride functionalized GNPs were dispersed into 0.02 M phosphate buffered saline (PBS) solution containing 5% glutaraldehyde for 2 h. Initial PBS buffer pH was kept as 7.4. After that, for anti-GD2 antibody immobilization, GNPs were incubated with anti-GD2 antibody for 16 h at 4 °C. At the end, anti-GD2 antibody conjugated GNPs were washed with PBS buffer several times to remove excess unconjugated anti-GD2 antibody. Next, we have used high-resolution JEM-2100F transmission electron microscope (TEM) and UV−visible absorption spectrum for the characterization of anti-GD2 antibody attached GNP as shown Figure S1A (see Supporting Information) and Figure 1C.

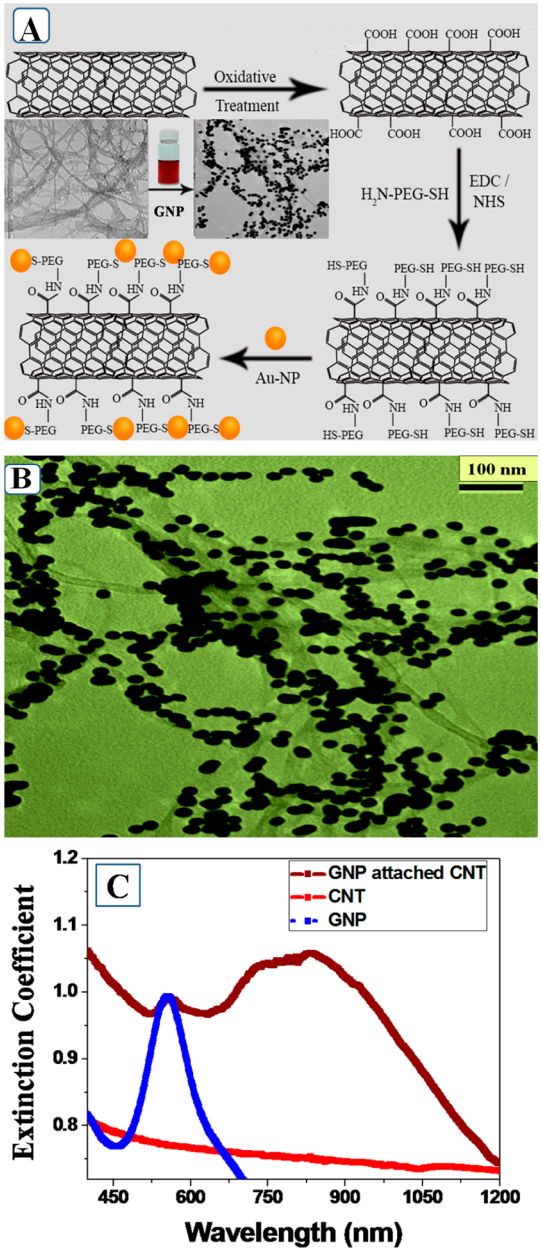

Figure 1. (A) Scheme showing the synthetic path we have followed for the development of gold nanoparticle attached theranostic SWCNT. (B) TEM data showing how gold nanoparticles are in assembly structure on GNP attached theranostic SWCNT. (C) Extinction spectra shows how the absorption features vary for carboxylic acid conjugated SWCNT, amine functionalized GNP, and theranostic GNP conjugated SWCNT material in water.

Synthesis of Anti-GD2 Antibody Attached Gold Nanoparticle Theranostic SWCNT. For the synthesis of theranostic SWCNT, at first, we have prepared water-soluble carboxy functionalized SWCNT. For this purpose, we have used nitric acid and sulfuric acid as strong oxidizing agent, as we have reported before.[8,23] During this process, SWCNT tips were chemically functionalized by carboxylic acid groups as shown in Figure 1A. Thiol PEG amine ($HS\text{-}PEG\text{-}NH_2$) was then added to the functionalized SWCNTs by treating the $-CO_2H$ in the presence of EDC (1-ethyl-3-(3-(dimethylamino)propyl)carbodiamide, HCl) cross-linking agent under inert medium. For this reaction, the coupling chemistry between $-CO_2H$ group of SWCNT and $-NH_2$ group of HS-PEG-

DOI: 10.1021/acsami.5b05225
ACS Appl. Mater. Interfaces 2015, 7, 20649−20656

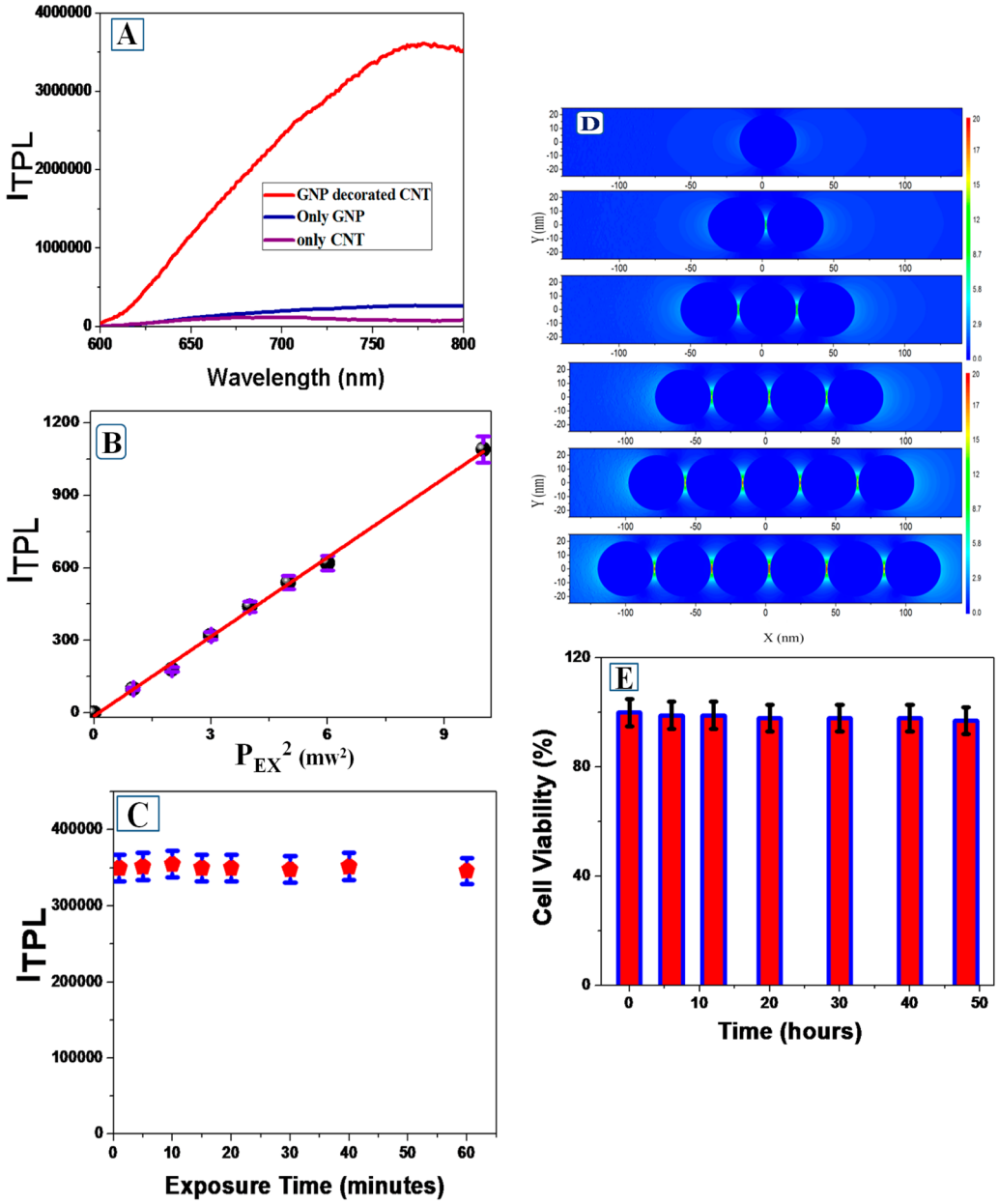

Figure 2. (A) Two-photon photoluminescence spectrum from anti-GD2 antibody conjugated SWCNT−GNP theranostic material, anti-GD2 antibody conjugated GNP, and anti-GD2 antibody conjugated SWCNT. NIR light (1100 nm) was used as the excitation source. (B) Plot indicates linear relationship between two-photon photoluminescence intensity at 775 nm from anti-GD2 antibody conjugated SWCNT−GNP theranostic material and the square of intensity of 1100 nm excitation laser power (P_{EX}). (C) Plot indicates two-photon luminescence at 775 nm from anti-GD2 antibody conjugated SWCNT−GNP remain same even after an hour of exposure with 1100 nm light. (D) Plot reports FDTD simulated electric field enhancement $|E|^2$ profiles (arb. unit) for nanoparticle assembly. For our calculation, we have used GNPs particle size as 40 nm, and separation distance between GNPs are kept as 3 nm. (E) Bar plot indicates very good biocompatibility of anti-GD2 antibody conjugated SWCNT−GNP theranostic against melanoma UACC903 cells. Even after 48 h incubation with 80 μg of hybrid material, we have observed about 97% cell viability.

NH_2 has been used to develop thiol PEG coupled SWCNT. For this purpose, carboxylated carbon nanotubes (10.0 mg) were dispersed in 50 mL of Millipore water. Then, 125.0 mg of EDC (1-ethyl-3-(3-(dimethylamino)propyl)carbodiamide, HCl) and 75.0 mg of NHS (*N*-hydroxysulfosuccinimide sodium salt) were mixed into the dispersed oxidized carbon nanotubes solution at room temperature. After that, 10 mL of MES buffer (zwitterionic N-substituted aminosulfonic acid, pH 6.1) was added slowly into the reaction mixture followed by sonication for 15 min. Then 5.0 mg of HS-PEG-NH_2 was added quickly to the solution, and the mixture was stirred slowly at room temperature for 6 h. The final product (amide-linked thiol-terminated (PEG-SH) carbon nanotubes) was washed thoroughly with water and collected by centrifugation (1000 rpm for 1 h). Figure S1B shows the morphology of water-soluble HS-PEG-NH_2 attached SWCNT. Figure S2A shows the FTIR spectra, where one can find the −SH and −CS stretching vibrations peaks at 2574 and 1058 cm^{-1}, respectively,[32] which indicate the conjugation of HS-PEG-NH2 with SWCNT. Similarly, we have observed amide vibration band for PEG amine attached SWCNT at ∼3250 cm^{-1}. The amide I band for PEG amine attached SWCNT was also observed at ∼1680 cm^{-1}.

In the next step, gold nanoparticles were conjugated with PEG coupled SWCNTs via the thiol group. At the end, unconjugated SWCNTS and nanoparticles were separated by centrifuge. FTIR spectrum as shown in Figure S2A clearly shows the disappearance of −SH vibration band, which can be attributed to the formation of Au−S bond as reported previously by Aryal et al.[32] The TEM image

DOI: 10.1021/acsami.5b05225
ACS Appl. Mater. Interfaces 2015, 7, 20649−20656

reported in the Figure 1B demonstrates that GNPs are nicely decorated on the surface of SWCNTs, and it is due to the formation of Au−S bond on the surface of SWCNT. Figure S4 shows the elemental mapping for theranostic SWCNTs which indicates that carbon, oxygen, and gold are present in hybrid materials.

Melanoma UACC903 Cells Culture and Incubation with Theranostic SWCNT Materials. We have obtained melanoma UACC903 cells, RPMI-1640 medium to grow melanoma cells and fetal bovine serum (FBS) from ATCC. We have grown melanoma cells in a carbon dioxide incubator in ATCC recommended medium. Experimental details have been reported before.[11,13,15] In the next step, we have measured the amount of GD2 in melonoma cells using an enzyme linked immunosorbent assay (ELISA) kit. After that, melanoma UACC903 cells at different concentrations were incubated with anti-GD2 antibody conjugated gold nanoparticle attached theranostic SWCNTs for the two-photon imaging and photothermal killing experiments.

Measurement Two-Photon Fluorescence Spectra from Anti-GD2 Antibody Conjugated GNP, SWCNT, and Theranostic Material. For the measurement of two-photon luminescence spectrum from antibody conjugated theranostic material, we have used 1100 nm NIR biological II window light from optical parametric amplifier (OPO), pumped by 100 fs pulse width and 80 MHz repetition rate Ti:sapphire laser (Coherent, U.S.A.) as an excitation source. To adjust the polarization of the incident light, we have used quarter wave plate and a polarizer before sample. For the separation of two-photon luminescence from the excitation and second harmonic light, TPL signal was passed through a 810 nm short-pass and 580 nm long-pass filter. At the end, TPL signal was recorded using CCD camera (Princeton Instrument) integrated with a monochromator.

Two-Photon Fluorescence Imaging of Theranostic SWCNT Attached Melanoma Cells. To perform the two-photon imaging experiment using anti-GD2 antibody conjugated gold nanoparticle attached theranostic SWCNT bind melanoma UACC903 cells, we have used multiphoton microscope (FV1000MPE) from NIKON. Experimental details for two-photon imaging of cells has been reported before.[5,15] We have used 1100 nm light for cancer cell multiphoton imaging experiments.

Finite Difference Time Domain (FDTD) Simulation. For electromagnetic wave calculations, we have used the FDTD simulation software package, as previously reported by us and other groups.[5,30,33,34] For our simulation, we have used absorbing boundary condition. In our calculation, we have kept the time scale as 4000 fs, the amplitude of electric field as 1 V/m, and mesh resolution as 0.001 nm.

Theranostic SWCNT Based Photothermal Killing of Melanoma UACC903 Cells Using 980 nm Light and Determination of the Killing Efficiency for Melanoma UACC903 Cells. In our photothermal therapy experiment using anti-GD2 antibody conjugated gold nanoparticle attached theranostic SWCNT bind melanoma UACC903 cells, we have used 980 nm light generated by a portable laser diode as an excitation light source. For photothermal killing experiments, the power of the diode laser generated 980 nm light was kept as 1 W/cm^2. After performing photothermal killing experiments for melanoma UACC903 cells, we have used typan blue and MTT assay to find the cell viability of melanoma UACC903 cells. Experimental details for typan blue and MTT assay were reported before[4,8,23]

RESULTS AND DISCUSSION

The SERS spectrum from theranostic SWCNTs as shown in Figure S3 shows two main bands. The first one is tangential Raman allowed optical mode E_{2g}, known as G band, which is centered around 1590 cm^{-1}. The second band is mainly due to the defect band, known as D band, which is centered around 1340 cm^{-1}.[8−10,22−24] Figure 1C reports the extinction spectra from water-soluble carboxylic acid conjugated SWCNTs, amine functionalized GNPs, and GNP conjugated SWCNTs, where GNPs are in assembly structure. Our observed structureless absorption features from water-soluble carboxylic acid conjugated SWCNTs is well documented in the literature.[8−10,22−24] E11 and E22 transitions of nanotubes are responsible for the observed structureless absorption features.[8−10,22−24] On the other hand, spherical GNPs show a strong plasmon band around 540 nm, which is well documented in the literature,[7,8,10,11,14] and it is due to the conduction band electrons oscillation.[7,8,10,11,14] As shown in Figure 1C, our experimental results showed that for the theranostic SWCNT material, the absorption features looks very broad, starting from 500 to 1200 nm. Since in case of theranostic SWCNT material GNPs are assembly structure on SWCNT surface, due to the strong plasmon coupling between plasmon frequency of each GNP, there is obvious increase in the extinction at longer wavelengths, which we have observed in Figure 1C.

Figure 2A reports the two-photon photoluminescence spectra from anti-GD2 antibody attached GNP−SWCNT theranostic, anti-GD2 antibody attached gold nanoparticle, and anti-GD2 antibody attached SWCNT, when we have used 1100 nm NIR light excitation. To find out whether the luminescence from anti-GD2 antibody attached SWCNT theranostic was observed is due to multiphoton excitation, we have performed power dependent experiments using NIR 1100 nm excitation wavelength. For this purpose, 775 nm luminescence intensities from theranostic SWCNTs were measured by varying the excitation power, as reported in the Figure 2B. Reported data confirm that the 775 nm luminescence intensity is indeed proportional to the square of the 1100 nm excitation laser power, which clearly indicates that our observed luminescence is due to two-photon excitation process. It is very interesting to note that experimental observation reported in the Figure 2A shows that the two-photon intensity from theranostic anti-GD2 antibody attached GNP conjugated SWCNT materials are about 6 orders of magnitude higher than that of anti-GD2 antibody attached GNP or anti-GD2 antibody attached SWCNT alone, which is highly remarkable. The observed very high two-photon fluorescence from anti-GD2 antibody attached GNP conjugated theranostic SWCNT is due to the fact that gold nanoparticles are in assembled nanostructures on the surface of theranostic SWCNT materials.

As a result, each GNP plasmon frequency undergoes strong coupling, which helps to amplify electromagnetic fields tremendously at the "hot spot", which we have also confirmed from theoretical simulation data. Due to the above fact, we have observed a very broad surface plasmon resonance band, as reported in Figure 1C. Recent report indicates that the possible mechanism for two-photon luminescence from gold atom can be due to the sequential absorption of two photons followed by recombination of an electron in the sp band and a hole in the d band.[17−24] Since in our experimental condition, 1100 nm excitation wavelength is in resonance with the anti-GD2 antibody attached GNP conjugated SWCNT theranostic material absorption spectra, during the excitation process, gold nanoparticle assembly attached SWCNTs are resonantly excited by 1100 nm light. Also, since the probability of two-photon absorption is proportional to the fourth power of the electric field enhancement, TPL intensity from anti-GD2 antibody attached GNP conjugated SWCNT theranostic materials is expected to have huge amplification when the local electric field is strong due to plasmon coupling.

DOI: 10.1021/acsami.5b05225
ACS Appl. Mater. Interfaces 2015, 7, 20649−20656

Next, we have performed FDTD simulation, for theoretical understanding on how TPL signal enhances, due to the local field generated by gold nanoparticle assembly via plasmon frequency coupling. Simulation details have been reported before.[5,30,32] In our theoretical calculation, we have used spherical GNP with 40 nm particle sizes. We have also kept separation distance between GNPs as 3 nm for our simulation calculation. During the calculation, multipolar and finite size effects, which are very important for the assembly structure, were incorporated. FDTD simulations results, as illustrated in Figure 2D, indicate more than 25 times of $|E|^2$ intensity enhancement for gold nanoassembly containing six particles in comparison to the monomer gold nanoparticle. As previously discussed, since the probability of two-photon absorption is proportional to the fourth power of the electric field enhancement, around 3 orders of magnitude enhancement of TPL intensity is expected for nanoassembly, just due the stronger electric field enhancement. So 6 orders of magnitude enhancement of TPL intensity for theranostic materials is mainly due to strong resonance enhancement coupled with the stronger electric field enhancement.

For multiphoton imaging of biomolecules like cancer cell, photostability and biocompatibility are the necessary conditions which need to be evaluated before anti-GD2 antibody conjugated SWCNT−GNP theranostic material can be used for multiphoton imaging purpose. As a result, we have performed photostability experiment for anti-GD2 antibody conjugated SWCNT−GNP theranostic. From the experimental data, as shown in Figure 2C, we can conclude that the photostability of the theranostic anti-GD2 antibody conjugated material is very good, and as result, we have observed that two-photon luminescence signals at 775 nm remain almost unchanged even after 60 min of exposure.

Next, to find out the biocompatibility of anti-GD2 antibody conjugated SWCNT-GNP theranostic material, we have tested cytotoxicity using melanoma UACC903 cells. For this purpose, 1.1×10^5 cells/mL of melanoma UACC903 cells were incubated with 80 μg of theranostic SWCNT material for different time intervals from 1 to 48 h. After that, we have used MTT test[4,10,11,26,27] to determine amount of live melanoma UACC903 cells. Our experimental data, as reported in Figure 2E, indicate that even after 48 h of incubation with 80 μg of theranostic SWCNT material, we have observed 97% of melanoma UACC903 cell viability.

We have also performed the same experiment with normal normal human skin cell line, HaCaT keratinocytes, where about 98% cell viability was noted even after 48 h of incubation with 80 μg of theranostic SWCNT material. Cytotoxicity results with normal and cancer cell lines clearly demonstrate good biocompatibility of our developed anti-GD2 antibody conjugated SWCNT-GNP theranostic materials.

All the above experimental data indicate that our developed anti-GD2 antibody conjugated SWCNT-GNP theranostic materials have very good TPL properties and that biocompatibility and photostability are quite good, which clearly shows that anti-GD2 antibody conjugated SWCNT-GNP hybrid materials can be promising candidates for NIR light induced two-photon luminescence microscopy imaging for melanoma UACC903 cells. For two-photon imaging of melanoma UACC903 cells, anti-GD2 antibody conjugated SWCNT−AuNP hybrid materials were incubated with different concentrations of melanoma UACC903 cells for 30 min. After that, unconjugated melanoma UACC903 cells were separated using centrifugation followed by washing with buffer several times to make sure that unconjugated melanoma UACC903 cells are completely separated from anti-GD2 antibody conjugated SWCNT−GNP hybrid bound melanoma cells. Figure 3A is a high-resolution TEM image which indicates

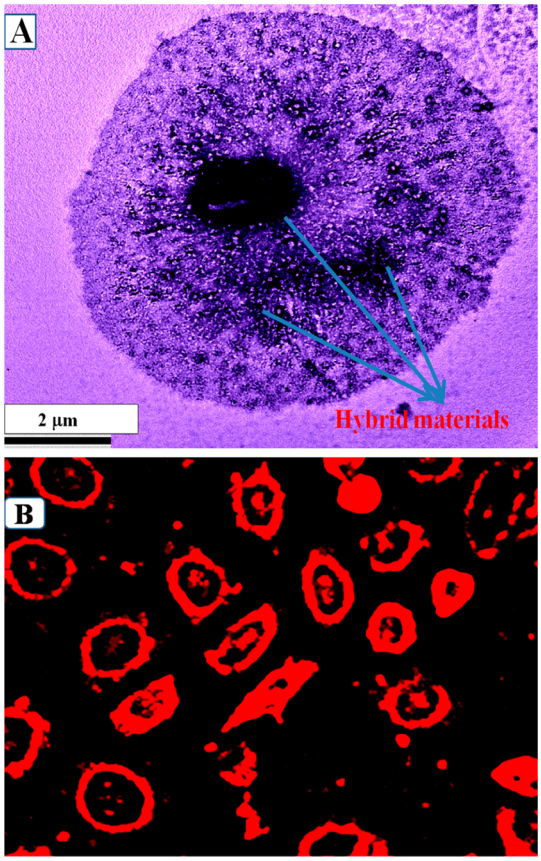

Figure 3. (A) TEM image showing single melanoma UACC903 cell is conjugated with SWCNT−GNP theranostic. (B) Two-photon luminescence image of anti-GD2 antibody conjugated SWCNT−GNP theranostic attached melanoma UACC903 cells. 1100 nm light was used as excitation source.

that single melanoma UACC903 cell is conjugated with anti-GD2 antibody conjugated SWCNT−GNP hybrid. Figures 3B show the two-photon luminescence image of melanoma UACC903 cell after binding with anti-GD2 antibody conjugated SWCNT-GNP hybrid. Bright two-photon imaging from melanoma UACC903 cells clearly demonstrate that anti-GD2 antibody conjugated hybrid material can be used for two-photon imaging of melanoma UACC903 cells in clinical environment. TPL imaging results, as shown in Figure 3B, indicate that not only are hybrid nanomaterials localized in the proximity of the cell membrane but also that they have penetrated through the cell membrane and localized inside the cell. It is now well documented[35,36] that SWCNT can be internalized into cells via either the classic endocytic or nonendocytotic pathways. For the hybrid material developed by us, due to the big size of GNP assembly on SWCNT surface, the endocytosis pathway will be the most probable path.

Next, to find out whether anti-GD2 antibody conjugated SWCNT-GNP hybrid based two-photon luminescence imaging is selective for melanoma UACC903 cell, anti-GD2 antibody conjugated SWCNT−GNP hybrids were incubated with 3.3 ×

DOI: 10.1021/acsami.5b05225
ACS Appl. Mater. Interfaces 2015, 7, 20649−20656

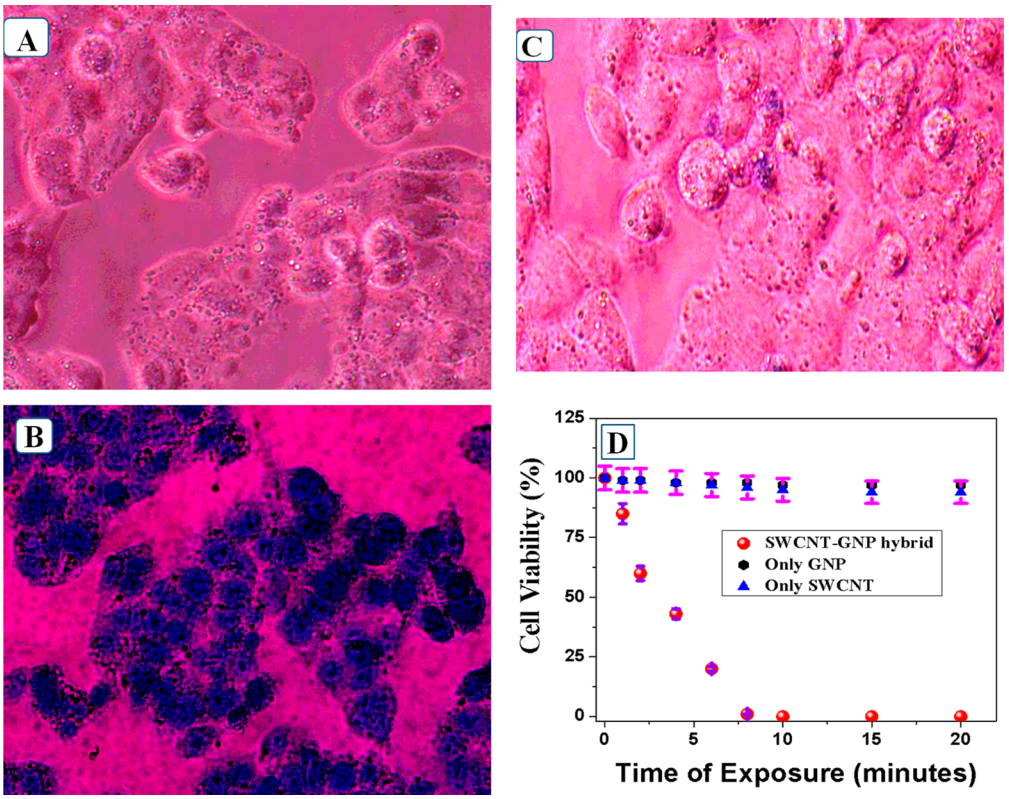

Figure 4. (A) Bright-field inverted microscopic images of melanoma UACC903 cells after 20 min of exposure by 980 nm light in the absence of anti-GD2 antibody conjugated SWCNT−GNP hybrid theranostic material. Reported data indicate that cancer cells are alive even after 20 min of 980 nm light exposure. (B) Bright-field inverted microscopic images of theranostic SWCNT attached melanoma UACC903 cells after irradiation with 980 nm near-IR biological II window at 1 W/cm^2 for 6 min. Reported data indicate that most melanoma UACC903 cancer cells are dead after 6 min of photothermal therapy. (C) Bright-field inverted microscopic images of melanoma UACC903 cells after 20 min exposure by 980 nm light in the presence of anti-GD2 antibody conjugated GNP. Reported data indicate that cancer cells are alive even after 20 min of 980 nm light exposure. (D) Plot illustrating the amount of cell viability measured using MTT test for different time intervals of exposure for anti-GD2 antibody conjugated SWCNT, anti-GD2 antibody conjugated GNP, and anti-GD2 antibody conjugated SWCNT−GNP hybrid theranostic material.

10^5 cells/mL normal skin HaCaT cells for 30 min. Two-photon fluorescence image as reported in Figures S5A−B indicates that anti-GD2 antibody conjugated SWCNT−GNP hybrid hybrid material based TPL imaging is selective for targeted melanoma UACC903 cancer cells.

After successful targeted two-photon imaging of melanoma UACC903 cell, we have performed NIR light induced photothermal killing of melanoma UACC903 cells in biological II window using 980 nm light from laser diode. Targeted photothermal experiments for melanoma UACC903 cells were performed using 1 W/cm^2 power NIR light. At first we have performed typan blue and MTT colorimetric assay[4,10,11,26,27] as shown in Figure 4 to determine the amount of live and dead melanoma UACC903 cells due to photothermal therapy using biological II window light. Our reported experimental bright-field inverted microscopic images of melanoma UACC903 cells, as illustrated in Figure 4B, demonstrated that most of the melanoma UACC903 cells are dead just after 6 min of 980 nm light triggered photothermal experiment. On the other hand, our experimental data, as reported in Figure 4A, show that in the absence of anti-GD2 antibody conjugated SWCNT-GNP hybrid material, most of the melanoma UACC903 cell is alive even after 20 min of exposure at 980 nm light.

Figure 4D shows the results of the MTT test; only 7% melanoma UACC903 cells were dead in the absence of anti-GD2 antibody conjugated SWCNT after 20 min of therapy experiment, whereas about 100% of cells were dead after 8 min of exposure in the case of theranostic material. Our experimental photothermal killing data reported in Figures 4C and 4D indicate that only 6% melanoma UACC903 cells were dead in the case of anti-GD2 antibody conjugated gold nanoparticle after 20 min of therapy experiment. Observed very efficient photothermal killing of melanoma UACC903 cells in the case of anti-GD2 antibody conjugated SWCNT−GNP hybrid is mainly because the theranostic nanomaterial has a very strong absorption peak at 980 nm as shown in Figure 1C. As we and others have reported before, heating properties of GNPs or their assemblies are based on surface plasmon resonances overlap with the excitation light source.[4,10,11,26,27] When anti-GD2 antibody conjugated GNP or anti-GD2 antibody conjugated GNP attached SWCNTs materials were illuminated by an electromagnetic field at 980 nm wavelength, heat was generated on the melanoma UACC903 cells surfaces due to the consequence of the relaxation of the light from excited surface via electron−phonon interactions.[4,10,11,26,27] This process leads to the heat-up of the surrounding chemically attached melanoma UACC903 cells. The main criteria for this to occur is that the 980 nm wavelength of light overlaps with the SPR absorption band. As shown in Figure 1C, since SWCNT absorption cross section is very low at 980 nm, the observed hypothermia effect is also low. Similarly, since anti-GD2 antibody conjugated gold nanoparticles do not exhibit any absorption at 980 nm, only 3−6% of cell death were observed.

DOI: 10.1021/acsami.5b05225
ACS Appl. Mater. Interfaces 2015, 7, 20649−20656

CONCLUSION

In the current article, we have reported plasmon coupling enhanced selective two-photon imaging and huge enhancement of photothermal killing of melanoma UACC903 cells in biological II NIR window using anti-GD2 antibody attached theranostic GNP conjugated SWCNTs. TPL measurement using 1100 nm biological II NIR window light indicates that two-photon intensities from the anti-GD2 antibody attached theranostic GNP conjugated SWCNT hybrid materials are almost 6 orders of magnitude higher than anti-GD2 antibody attached GNP or anti-GD2 antibody attached SWCNTs, which is highly remarkable. Experimental measurements with FDTD simulations indicate that 6 orders of magnitude enhancement of TPL intensity for anti-GD2 antibody attached theranostic GNP conjugated SWCNT hybrid materials is mainly due to strong resonance enhancement in plasmon frequency coupled with the stronger electric field enhancement. Reported experimental observation shows that long-time photostability and cellular biocompatibility are very good for anti-GD2 antibody attached theranostic material. Reported experimental observation shows that anti-GD2 antibody attached theranostic material based two-photon luminescence platforms are very selective for TPL imaging of melanoma UACC903 cells in the second biological NIR windows. The capability for bright TPL imaging of selective cancer cells, photostability, and biocompatibility makes theranostic material a good candidate for TPL imaging material for cancer.

Selective biological II window NIR light triggered photothermal killing experimental data show that about 100% melanoma UACC903 cells were dead after just 8 min of exposure in the case of anti-GD2 antibody attached theranostic GNP conjugated SWCNT hybrid theranostic material, whereas reported experimental data indicate that less that 10% of cells were dead in the presence of anti-GD2 antibody attached GNP or anti-GD2 antibody attached SWCNT alone. Reported experimental data demonstrate that due to coupling of plasmon frequency, the anti-GD2 antibody attached theranostic material serves as a photothermal source through nonradiative decay and is also able to act as a local nanoantennae to enhance the optical energy absorption of anti-GD2 antibody attached theranostic GNP conjugated nanomaterials. Observed highly enhanced photothermal effects using anti-GD2 antibody attached theranostic GNP conjugated theranostic material in second biological NIR window can have real life applications for cancer therapy in clinical environment.

ASSOCIATED CONTENT

Supporting Information

The Supporting Information is available free of charge on the ACS Publications website at DOI: 10.1021/acsami.5b05225.

Detailed characterizations and other experiments (PDF)

AUTHOR INFORMATION

Corresponding Author

*E-mail: paresh.c.ray@jsums.edu. Fax: +160197936.

Notes

The authors declare no competing financial interest.

ACKNOWLEDGMENTS

P.C.R. thanks NSF-PREM, grant no. DMR-1205194, for their generous funding. We also thank NIH RCMI, grant no. G12MD0007581, for Molecular and Cellular Biology and Analytic Laboratory Core facilities.

REFERENCES

(1) Van Denderen, B. J. E.; Thompson, E. W. Cancer: The to and fro of Tumour Spread. *Nature* **2013**, *493*, 487−488.

(2) Lim, E. K.; Kim, T.; Paik, S.; Haam, S.; Huh, Y. M.; Lee, K. Nanomaterials for Theranostics: Recent Advances and Future Challenges. *Chem. Rev.* **2015**, *115*, 327−39.

(3) Dreaden, E. C.; Alkilany, A. M.; Huang, X.; Murphy, C. J.; El-Sayed, M. A. The Golden Age: Gold Nanoparticles for Biomedicine. *Chem. Soc. Rev.* **2012**, *41*, 2740−2779.

(4) Fan, Z.; Senapati, D.; Singh, A. K.; Ray, P. C. Theranostic Magnetic Core−Plasmonic Shell Star Shape Nanoplatform for the Isolation of Targeted Rare Tumor Cells from Whole Blood, Fluorescence Imaging, and Photothermal Destruction of Cancer. *Mol. Pharmaceutics* **2013**, *10*, 857−866.

(5) Demeritte, T.; Fan, Z.; Sinha, S. S.; Duan, J.; Pachter, R.; Ray, P. C. Gold Nanocage Assembly for Selective Second Harmonic Generation Imaging of Cancer Cell. *Chem.—Eur. J.* **2014**, *20*, 1017−1022.

(6) Liu, X.; Wang, S. Three-Dimensional Nano-Biointerface as a New Platform for Guiding Cell Fate. *Chem. Soc. Rev.* **2014**, *43*, 2385−2401.

(7) Fan, Z.; Shelton, M.; Singh, A. K.; Senapati, D.; Khan, S. A.; Ray, P. C. Multifunctional Plasmonic Shell−Magnetic Core Nanoplatforms for Targeted Diagnostics, Isolation, and Photothermal Destruction of Tumor Cells. *ACS Nano* **2012**, *6*, 1065−1073.

(8) Beqa, L.; Fan, Z.; Singh, A. K.; Senapati, D.; Ray, P. C. Gold Nano Popcorn Attached SWCNT Hybrid Nanomaterial for Targeted Diagnosis and Photothermal Therapy of Human Breast Cancer Cells. *ACS Appl. Mater. Interfaces* **2011**, *3*, 3316−3324.

(9) Yoon, H. J.; Kozminsky, M.; Nagrath, S. Emerging Role of Nanomaterials in Circulating Tumor Cell Isolation and Analysis. *ACS Nano* **2014**, *8*, 1995−2017.

(10) Lu, W.; Singh, A. K.; Khan, S. A.; Senapati, D.; Yu, H.; Ray, P. C. Gold Nano-Popcorn-Based Targeted Diagnosis, Nanotherapy Treatment, and In Situ Monitoring of Photothermal Destruction Response of Prostate Cancer Cells Using Surface-Enhanced Raman Spectroscopy. *J. Am. Chem. Soc.* **2010**, *132*, 18103−18114.

(11) Huang, X.; El-Sayed, I. H.; Qian, W.; El-Sayed, M. A. Cancer Cell Imaging and Photothermal Therapy in the Near-Infrared Region by Using Gold Nanorods. *J. Am. Chem. Soc.* **2006**, *128*, 2115−2120.

(12) Robinson, J. T.; Hong, G.; Liang, Y.; Zhang, B.; Yaghi, O. K.; Dai, H. In vivo Fluorescence Imaging in the Second Near-Infrared Window with Long Circulating Carbon Nanotubes Capable of Ultrahigh Tumor Uptake. *J. Am. Chem. Soc.* **2012**, *134*, 10664−10669.

(13) Multifunctional Hybrid Graphene Oxide for Label-Free Detection of Malignant Melanoma from Infected Blood. Kanchanapally, R.; Fan, Z.; Singh, A. K.; Sinha, S. S.; Ray, P. C. Multifunctional hybrid graphene oxide for label-free detection of malignant melanoma from infected blood. *J. Mater. Chem. B* **2014**, *2*, 1934−1937.

(14) Yuan, P.; Ma, R.; Guan, Z.; Gao, N.; Xu, Q. H. Tuning Two-Photon Photoluminescence of Gold Nanoparticle Aggregates with DNA and Its Application as Turn-on Photoluminescence Probe for DNA Sequence Detection. *ACS Appl. Mater. Interfaces* **2014**, *6*, 13149−13156.

(15) Pramanik, A.; Chavva, S. R.; Fan, Z.; Sinha, S.; Nellore, B. P.; Ray, P. C. Extremely High Two-Photon Absorbing Graphene Oxide for Imaging of Tumor Cells in the Second Biological Window. *J. Phys. Chem. Lett.* **2014**, *5*, 2150−2154.

(16) Mujoo, K.; Cheresh, D. A.; Yang, H. M.; Reisfeld, R. A. Disialoganglioside GD2 on Human Neuroblastoma Cells: Target Antigen for Monoclonal Antibody-Mediated Cytolysis and Suppression of Tumor Growth. *Cancer Res.* **1987**, *47*, 1098−1104.

(17) Durr, N. J.; Larson, T.; Smith, D. K.; Korgel, B. K.; Sokolov, K.; Ben-Yakar, A. Two-photon Luminescence Imaging of Cancer Cells Using Molecularly Targeted Gold Nanorods. *Nano Lett.* **2007**, *7*, 941−945.

DOI: 10.1021/acsami.5b05225
ACS Appl. Mater. Interfaces 2015, 7, 20649−20656

(18) Punj, D.; Mivelle, M.; Moparthi, S. B.; van Zanten, T. S.; Rigneault, H.; van Hulst, N. F.; García-Parajó, M. F.; Wenger, J. A Plasmonic 'Antenna-in-Box' Platform for Enhanced Single-Molecule Analysis at Micromolar Concentrations. *Nat. Nanotechnol.* **2013**, *8*, 512−516.
(19) Wissert, M. D.; Ilin, K. S.; Siegel, M.; Lemmer, U.; Eisler, H. J. Coupled Nanoantenna Plasmon Resonance Spectra from Two-Photon Laser Excitation. *Nano Lett.* **2010**, *10*, 4161−4165.
(20) Guan, Z.; Gao, N.; Jiang, X. F.; Yuan, P.; Han, F.; Xu, Q. H. Huge Enhancement in Two Photon Photoluminescence of Au Nanoparticle Clusters Revealed by Single Particle Spectroscopy. *J. Am. Chem. Soc.* **2013**, *135*, 7272−7277.
(21) Kinkhabwala, A.; Yu, Z. F.; Fan, S. H.; Avlasevich, Y.; Mullen, K.; Moerner, W. E. Large Single-Molecule Fluorescence Enhancements Produced by a Bowtie Nanoantenna. *Nat. Photonics* **2009**, *3*, 654−657.
(22) Zhao, T.; Yu, K.; Li, L.; Zhang, T.; Guan, Z.; Gao, N.; Yuan, P.; Li, S.; Yao, S. Q.; Xu, Q.-H.; Xu, G. Q. Gold Nanorod Enhanced Two-Photon Excitation Fluorescence of Photosensitizers for Two-Photon Imaging and Photodynamic Therapy. *ACS Appl. Mater. Interfaces* **2014**, *6*, 2700−2708.
(23) Khan, S. A.; Kanchanapally, R.; Fan, Z.; Beqa, L.; Singh, A. K.; Senapati, D.; Ray, P. C. A Gold Nanocage−CNT Hybrid for Targeted Imaging and Photothermal Destruction of Cancer Cells. *Chem. Commun.* **2012**, *48*, 6711−6713.
(24) Wang, X.; Wang, C.; Cheng, L.; Lee, S. T.; Liu, Z. Noble Metal Coated Single-Walled Carbon Nanotubes for Applications in Surface Enhanced Raman Scattering Imaging and Photothermal Therapy. *J. Am. Chem. Soc.* **2012**, *134*, 7414−7422.
(25) http://www.cancernetwork.com/cancermanagement/melanoma-and-other-skin-cancers, date of access 01/12/2015.
(26) Wang, C.; Xu, L.; Liang, C.; Xiang, J.; Peng, R.; Liu, Z. Immunological Responses Triggered by Photothermal Therapy with Carbon Nanotubes in Combination with Anti-CTLA-4 Therapy to Inhibit Cancer Metastasis. *Adv. Mater.* **2014**, *26*, 8154−8162.
(27) Liu, J.; Wang, C.; Wang, X.; Wang, X.; Cheng, L.; Li, Y.; Liu, Z. Mesoporous Silica Coated Single-Walled Carbon Nanotubes as a Multifunctional Light-Responsive Platform for Cancer Combination Therapy. *Adv. Funct. Mater.* **2015**, *25*, 384−392.
(28) Liang, H.; Zhang, X. B.; Lv, Y.; Gong, L.; Wang, R.; Zhu, X.; Yang, R.; Tan, W. Functional DNA-Containing Nanomaterials: Cellular Applications in Biosensing, Imaging, and Targeted Therapy. *Acc. Chem. Res.* **2014**, *47*, 1891−190.
(29) Pérez-Hernández, M.; Pino, P. D.; Mitchell; María, S. G.; Stepien, G.; Pelaz, B.; Parak, W. J.; Gálvez, E. M.; Pardo, J.; de la Fuente, J. M. Dissecting the Molecular Mechanism of Apoptosis during Photothermal Therapy Using Gold Nanoprisms. *ACS Nano* **2015**, *9*, 52−61.
(30) Sinha, S. S.; Paul, D. K.; Kanchanapally, R.; Pramanik, A.; Chavva, S. R.; Nellore, B. P. V.; Jones, S. J.; Ray, P. C. Long-range Two-photon Scattering Spectroscopy Ruler for Screening Prostate Cancer Cells. *Chem. Sci.* **2015**, *6*, 2411−2418.
(31) Huang, S.-C.; Caldwell, K. D.; Lin, J.-N.; Wang, H.-K.; Herron, J. N. Site-Specific Immobilization of Monoclonal Antibodies Using Spacer-Mediated Antibody Attachment. *Langmuir* **1996**, *12*, 4292−4298.
(32) Aryal, S.; Remant, B. K. C.; Dharmaraj, N.; Bhattarai, N.; Kim, C. H.; Kim, H. Y. Spectroscopic Identification of S Au Interaction in Cysteine Capped Gold Nanoparticles. *Spectrochim. Acta, Part A* **2006**, *63*, 160−163.
(33) Yan, Y.; Li, L.; Feng, C.; Guo, W.; Lee, S.; Hong, M. Microsphere-Coupled Scanning Laser Confocal Nanoscope for Sub-Diffraction-Limited Imaging at 25 nm Lateral Resolution in the Visible Spectrum. *ACS Nano* **2014**, *8*, 1809−1816.
(34) Zhao, J.; Pinchuk, A. O.; McMahon, J. M.; Li, S.; Ausman, L. K.; Atkinson, A. L.; Schatz, G. C. Methods for Describing the Electromagnetic Properties of Silver and Gold Nanoparticles. *Acc. Chem. Res.* **2008**, *41*, 1710−1720.
(35) Kostarelos, K.; Lacerda, L.; Pastorin, G.; Wu, W.; Wieckowski, S.; Luangsivilay, J.; Godefroy, S.; Pantarotto, D.; Briand, J. P.; Muller, S.; Prato, M.; Bianco, A. Cellular Uptake of Functionalized Carbon nanotubes is Independent of Functional Group and Cell Type. *Nat. Nanotechnol.* **2007**, *2*, 108−113.
(36) Bhattacharya, S.; Roxbury, D.; Gong, X.; Mukhopadhyay, D.; Jagota, A. DNA Conjugated Swcnts Enter Endothelial Cells via Rac1Mediated Macropinocytosis. *Nano Lett.* **2012**, *12*, 1826−1830.

DOI: 10.1021/acsami.5b05225
ACS Appl. Mater. Interfaces 2015, 7, 20649−20656